Computer-Aided Liner Optimization For Broadband Noise

L. Lafronza * and A. McAlpine, †
A.J. Keane ‡ and R.J. Astley , §
Computational Engineering Design Group,
Institute of Sound and Vibration Research,
University of Southampton, Southampton SO17 1BJ, UK.

In this article the attenuation of broadband noise in an acoustically-lined circular-section duct is investigated. The aim is to predict how an axially segmented liner influences the attenuation of broadband noise in an aero-engine intake. The sound field is modelled using a multi-modal representation, assuming an ensemble of uncorrelated modes over a wide range of frequencies. An optimization procedure based on a Response Surface Model is used to investigate the optimum uniform and axially-segmented acoustic liner that maximizes the attenuation of broadband noise. An approximate calculation of the Perceived Noise Level (PNL) is used for the objective function. In this article the benefit of using an axially-segmented liner instead of a uniform liner to attenuate broadband noise is demonstrated.

Nomenclature

ρ_0	base flow density
p_0	base flow pressure
$\mathbf{u}_0$	base flow velocity
Z	liner impedance
R	liner resistance
X_m	liner mass reactance
X_c	liner cavity reactance
d	liner sheet hole diameter, m
n_o	number of liner sheet holes
σ	liner sheet porosity
h	liner thickness, m
k	wave number, rad m^{-1}
k_x	axial wave number, rad m^{-1}
k_r	radial wave number, rad m^{-1}
n	radial mode number
m	azimuthal mode number
β_{mn}	cut-off ratio
J_m	Bessel function of the first kind of order m
p'	acoustic pressure, Pa
b	duct radius, m
L	total axial liner length, m
M	Mach number
I_x	modal acoustic intensity in the axial direction

*Graduate Student,ISVR-CEDC, lorenzo@soton.ac.uk.
†Dr,ISVR, am@isvr.soton.ac.uk.
‡Professor,School of Engineering Sciences, Andy.Keane@soton.ac.uk
§Professor,ISVR, rja@isvr.soton.ac.uk

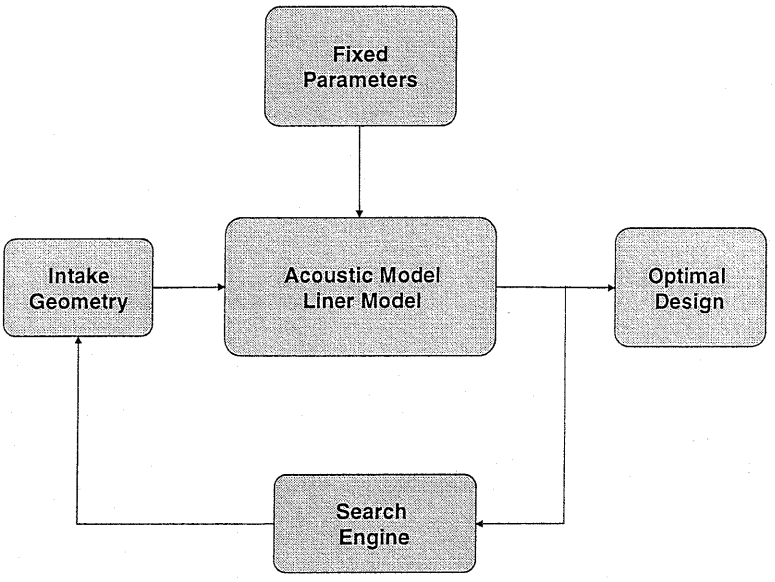

Figure 2. General optimization process.

centre frequencies to calculate the objective function (or cost function), which in this case is a Perceived Noise Level (PNL) algorithm.

Next an appropriate search is conducted with liner design variables R_i, h_i and l_i. The aim is to maximize $\Delta\text{PNL} = \text{PNL}_{hw} - \text{PNL}_{sw}$, the difference between the PNL in a hard-walled duct and that in the lined duct. In this case the optimization software package *Options* has been used to drive the acoustic solution to the best conceptual design.[10]

III. Acoustic Model

In the following analysis the intake is modelled as a duct of uniform circular cross-section with a uniform mean-flow at Mach number $M < 1$. The acoustic propagation model is based on the linearized set of equations governing the isentropic motion of a non-viscous, non-heat-conducting perfect gas.[4] The linearized acoustic equations are obtained by considering small perturbations to a mean state ρ_0, p_0 and $\mathbf{u}_0 = u_0\mathbf{i}$. It is assumed that an unspecified noise source introduces harmonic disturbances with time dependence $e^{i\omega t}$, where $\omega = 2\pi f$ is the excitation frequency. The resulting acoustics fluctuations in the duct can then be written $p = p'e^{i\omega t}$, where p' now satisfies the convected Helmholtz equation. In cylindrical polar coordinates (r, θ, x) it is well know that on separating the variables r, θ and x the acoustic pressure can be expressed as a Fourier–Bessel modal sum and each element will be of form

$$p'_{mn} = A_{mn} J_m(k_{r_{mn}} r) e^{i[m\theta - k_{x_{mn}} x]}, \tag{2}$$

where $k_{x_{mn}}$ and $k_{r_{mn}}$ are the axial and radial wavenumbers for the mth circumferential mode and nth radial mode, J_m is the Bessel function of the first kind of order m and A_{mn} is a constant. The radial wavenumbers $k_{r_{mn}}$ are determined by application of the boundary condition and then solving the resulting eigenvalue equation.[4] Then $k_{x_{mn}}$ is given by

$$k_{x_{mn}} = \frac{k}{1 - M^2} \left[-M \pm \sqrt{1 - \left(\frac{1}{\beta_{mn}}\right)^2} \right], \tag{3}$$

where β_{mn} is the cut-off ratio,

$$\beta_{mn} = k \Big/ k_{r_{mn}} \sqrt{1 - M^2} \,. \tag{4}$$

The cut-off ratio defines which mode is propagating ($\beta_{mn} > 1$) and which is decaying ($\beta_{mn} \leq 1$), or as in the paper by Rice[11] we can say that a spinning mode is highly propagating (large β_{mn}) when the acoustic wave motion is mainly in the axial direction, while near cutoff ($\beta_{mn} \to 1$) the wave motion is mainly transverse or circumferential. Then it follows that the axial wavenumber k_x (3), associated with the mode (m, n), is real for $\beta_{mn} > 1$ and complex for $\beta_{mn} < 1$. It can be shown that the so called cut-off modes do not transmit any acoustic power since they are decaying modes.

For a multi-mode calculation a realistic assumption is that all the cut-on modes are uncorrelated, carrying equal sound power. Therefore at the fan plane, for a fixed frequency, all the cut-on modes have equal power. The transmission of each mode is then calculated separately. To assess the sound power transmitted by the modal pressure field it is necessary to take into account the mean flow. In Morfey[12] the following definition of acoustic intensity, valid for any flow which is isentropic and irrotational, is given:

$$I_{x_{mn}} = \frac{|p'|^2}{2\rho_0 c_0} \left((1 + M^2) Re(\beta_{mn}) + M(1 + |\beta_{mn}|^2) \right) . \tag{5}$$

Thus the sound power W of a single mode, in terms of the modal pressure amplitude A_{mn}, is found by integrating $I_{x_{mn}}$ over the duct cross-section. Using the orthogonal property of the Bessel function the integration yields,

$$W_{mn} = \frac{\pi}{2\rho_0 c_0} \left(b^2 - \frac{m}{k^2_{r_{mn}}} \right) |J_m(k_{r_{mn}} b)|^2 |A_{mn}|^2 \left((1 + M^2) Re(\beta_{mn}) + M(1 + |\beta_{mn}|^2) \right) . \tag{6}$$

The power W_{mn} is given by the sound power divided by the number of cut-on modes (at each frequency). Thus from Eq. (6) the amplitude A of a single incoming mode (m, n) can be found. The total sound power is constant at each frequency (white noise).

A key problem for this kind of broadband noise calculation arises when a phase angle for each mode has to be defined. In this case the propagating mode are assumed to be uncorreleted, but a better understanding of the phase acoustic source would be desirable.

IV. Mode-Matching theory

In an axisymmetric duct containing a finite length of acoustic lining there will be scattering where there is a change in the acoustic impedance at the duct wall. There is no scattering between azimuthal modes but only among different radial modes, this is because the impedance is uniform in the circumferential direction. Therefore an appropriate scheme to relate the sound field in the different regions in the duct has to be used. In order to take account of modal scattering, a mode-matching formulation is used.[8,9] The acoustic pressure at each axial position is written as a superposition of Fourier–Bessel modes

$$p'(x, r, \theta) = \sum_{m,n} J_m(k_{r_{mn}} r) e^{im\theta} \left[A^+_{mn} e^{-ik^+_{x_{mn}} x} + A^-_{mn} e^{-ik^-_{x_{mn}} x} \right] \tag{7}$$

where the superscripts $\pm$ are associated with waves propagating in the positive or negative (reflected mode) x-directions respectively. Note that the radial and axial wavenumbers take different values in the different regions of the duct (hard and lined). Similarly assuming the particle axial velocity is

$$u'_{x_{mn}}(x, r, \theta) = J_m(k_r\, r) e^{im\theta} \left[B^+_{mn} e^{-ik^+_{x_{mn}} x} + B^-_{mn} e^{-ik^-_{x_{mn}} x} \right] , \tag{8}$$

(using the same notation as above), from the acoustic momentum equation it can easily be shown that

$$B^\pm = \frac{k^\pm_x}{\rho_0(\omega - k^\pm_x u_0)} A^\pm . \tag{9}$$

For a fixed azimuthal mode m, at the interface between two different regions in the duct the continuity of pressure and axial particle velocity must be satisfied, that is

$$\int_{r=0}^{r=b} r\, J_m(k_{r_{mn}} r) \left\{ \begin{bmatrix} p'^{(j)} \\ u'^{(j)}_x \end{bmatrix} - \begin{bmatrix} p'^{(j+1)} \\ u'^{(j+1)}_x \end{bmatrix} \right\} \mathrm{d}r. \tag{10}$$

For all the radial modes this yields a system of $4\,N_r$ unknowns $(A^{\pm}_{mn}, B^{\pm}_{mn})$, with $2\,N_r$ equations at each interface. Now applying Eq. (10) at each interface j and using the relation (9) the system to solve can be written as

$$V \begin{bmatrix} A^{+}_{(j)} \\ A^{-}_{(j+1)} \end{bmatrix} = U \begin{bmatrix} A^{+}_{(j+1)} \\ A^{-}_{(j)} \end{bmatrix}, \tag{11}$$

where V and U are matrices. The subscript j denotes the duct section, and the vectors $A^{\pm}$ are of length N_r. To avoid problems associated with ill-conditioning an iterative procedure[8] is used to solve Eq. (11). In this case the duct is assumed to be anechoically terminated, so there are no reflected modes in the outlet section, (i.e. $B^{-}_{N+1} = 0$). The amplitudes of the incoming modes are all known (equal energy per mode). Therefore the transmission of each mode, specified by (m, n), can be calculated separately by using this mode-matching technique.

V. Optimization methods

The potential benefit of increased broadband noise attenuation with an axially varying liner compared with a uniform liner is examined. Two different optimization studies have been conducted.

First a uniform liner is studied using only two design variables to specify the acoustic lining, resistance R and liner depth h. Therefore a complete search of the 2D space, i.e. the (R, h)-plane, is performed, mapping all the possible configurations. When the number of variables increases a more sophisticated and efficient optimization procedure can be used. Several techniques are available, however for this kind of problem all these methods are time-consuming when the objective function is expensive to calculate. This means that the number of simulations (objective function evaluations) used to generate a suitable design is an important issue.[13] A relatively new optimization method is to build a surrogate model, and search this model instead. A Response Surface Model (RSM) is used here. First by running the simulations at a set of points (experimental design) and fitting response surfaces to the resulting input-output data, we obtain fast surrogates for the objective and constraint (if there are any) functions, that can be used for optimization, as explained by Jones[6] and Keane.[10]

The basic RSM process involves selecting a limited number of points at which the numerical simulations will be run, normally using formal DoE (Design of Experiments) methods.[5] Then, when these simulations have been performed, usually in parallel, a response surface (curve fit) is constructed through or near the data. Design optimization is then carried out on this surface to locate potential combinations of the design variables (that appear to minimize the cost function), which may then be fed back into the full code. These data points can then be used to update the model, and the whole process is repeated until some form of convergence is achieved, or an acceptable design has been obtained.

There are a number of variations and refinements that may be applied to the basic RSM approach. Here the general approach used takes an LPτDoE (sequence of initial points), and then a kriging approach is applied to build the RSM. Most DoE methods seek to sample the entire design space by building an array of possible designs with relatively even but not constant spacing between the points. A particular advantage of the LPτDoE approach is that not only does it give good coverage for engineering design purposes, but that it also allows additional points to be added to a design without the need to reposition existing points. Then if the initial build of the RSM is found to be inadequate, a new set of points can be inserted without invalidating the statistical character of the experiments. After the array of data points is built – from which a surface can be constructed – a decision has to be made whether to regress (as opposed to interpolate) the data. In this case the RSM model is built using a kriging approach. This methods allows the user to control the amount of regression (error source) as well as providing a theoretically sound basis for judging the degree of curvature needed to adequately model the user's data. Kriging also provides measures of probable errors in the model being built that can be used when assessing where to place any further points. Here a two stage search, genetic algorithm (*GA*) and a gradient descent (*DHC*), of the likelihood function has been carried out to tune the hyper parameters that define the kriging RSM. Finally a similar two stage search has been carried out on the RSM itself to find a new set of points that will be added to the database of sample points used to build the RSM. This process is shown in Fig. 3.

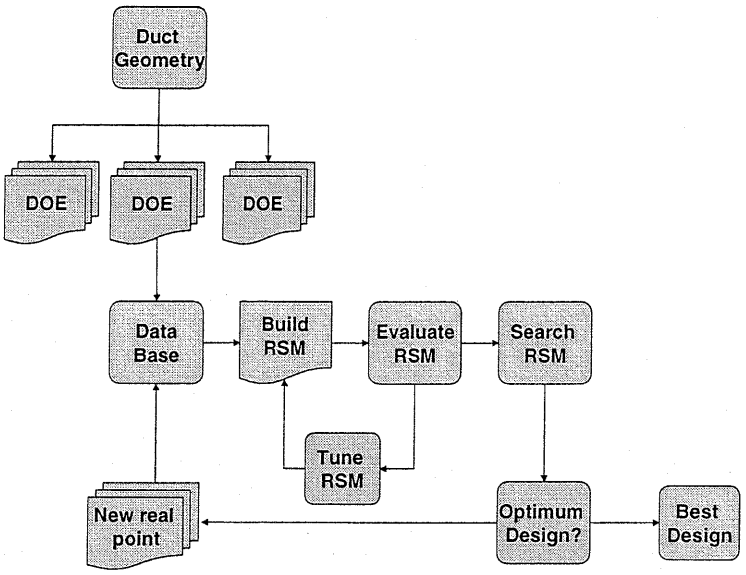

Figure 3. RSM-based optimization strategy.

VI. Results

The principal aim of this work is to demonstrate a liner design optimization procedure for broadband noise. The theory used to describe the physics of the problem and the optimization methodology has been described in the previous sections. To summarize, the noise source is approximated by assuming that at each frequency the incident sound field is formed by an uncorrelated ensemble of cut-on modes (equal energy per mode), and the intake is modelled as a duct of constant circular cross-section with a uniform mean-flow.

An optimization study has been conducted based on a idealized turbofan engine intake. The mean flow, and the fan's blade passing frequency (BPF) are based on a realistic flight condition (high engine power). The liner design variables, resistance R and liner depth h, are searched over the range $R = [1, 5]$ and $h = [6, 60]$ mm. In the numerical simulations the spectrum includes frequencies up to $\sim$ 2BPF. In this range only a discrete number of frequencies are used, these are the first eighteen third-octave centre frequencies. The objective function is given by an approximate evaluation of the Perceived Noise Level, based on the in-duct sound power at each third-octave centre frequency.

The optimization has involved a search with an initial base of 150 design points generated with LPτDoE distribution and evaluated in parallel. Then a series of optimizations, using a two stage search *GA* and *DHC*, has been used on the response surface model that is built from these initial points. The data point update to build a new RSM surface is conducted in two steps. First for each update of the database 10 new points are added to the initial DoE data set (parallel computation is used). When the design space has been comprehensively covered, and the location of the optimum point (or points) has been achieved to some specified confidence level, a new search is conducted. A double optimization process is used, first the hyper-parameters that define the kriging RSM are tuned to best fit the data, then the RSM is searched to find the optimum designs.

In Fig. 4 the optimization strategy used is shown plotting all the design variables combination used to sample and search the design space. In the upper-right-part of the figure all the combination between the different design variables in the first step (DoE) of the optimization are reported, this shown how the space has been covered uniformly. In the lower-left-part of Fig. 4 a kind of convergence history of the optimum found searching the meta-model is shown. It is clear how the search after few evaluation is restricted to a limited region of the design space, where the best design lies.

In Fig. 5 the ΔPNL contour map for a uniform liner configuration is shown. The plot includes the

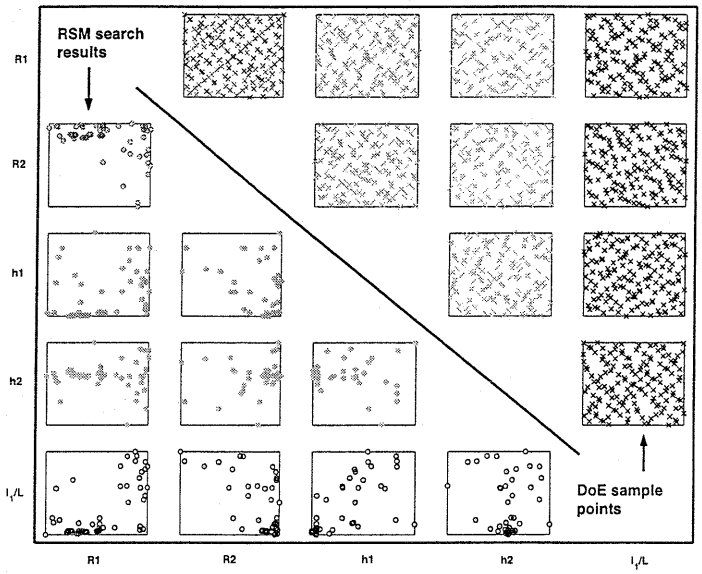

Figure 4. DoE sample distribution — RSM optimum search location.

optimum value that maximizes the difference between the PNL for a hard-walled duct and a lined 'soft-walled' duct (i.e. $\Delta\text{PNL} = \text{PNL}_{hw} - \text{PNL}_{sw}$). With a uniform lining the optimum liner design (full scale engine) is $R = 4$ and $h = 4\,\text{cm}$. The attenuation at the optimum is $\Delta\text{PNL} = 1.5\,\text{dB}$.

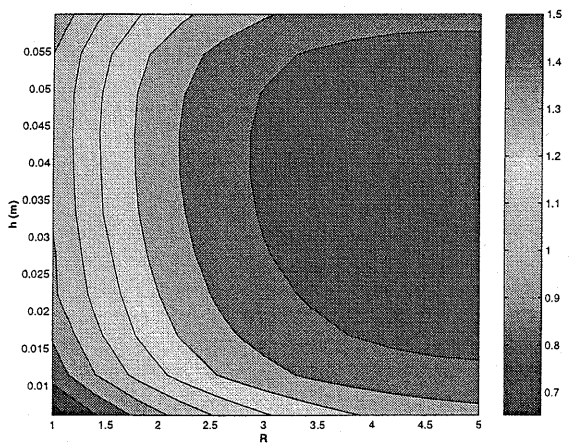

Figure 5. ΔPNL [dB] — uniform liner.

In Fig. 6 a 5D hierarchical axes technique (HAT) plot is shown. This plot contains most of the information needed to analyse the axially-varying liner optimization. Each part of the plot is associated with a different length of liner 1, i.e. different ratios of l_1/L. The variation of ΔPNL with resistance (R_1 and R_2) and liner depth (h_1 and h_2) is shown. Note that each individual tile in the plots has horizontal and vertical axis h_1 and h_2 respectively. Each of the subplots are a 4D HAT plot where the individual tiles are again a contour plots ($\Delta\text{PNL} = \Delta\text{PNL}(h_1, h_2)$) for a discrete value of the resistance (R_1, R_2) at a fixed value of l_1/L. All the plots are on the same colour scale.

Several different optimum values can be located in the design space at different liner configuration. A liner configuration for which the objective function (ΔPNL) is maximized can be interpolated from Figs. 6, 7 and 8, where the optimum for resistance, depth and liner length are plotted. The Fig. 9 also shows

how the relative liner length influences the variation of ΔPNL, this behaviour can also be observed in the 5DHAT 6 plot going from one tile to the other at fixed values of design variables.

With an axially-segmented liner the optimum design (full scale engine) is $R_1 = 3.5, R_2 = 4.5, h_1 = 1.5\text{cm}, h_2 = 4.3\text{cm}$ and $l_1/L = 10\%$. The maximum attenuation achivied at the optimum is $\Delta\text{PNL} = 2.0\,\text{dB}$, an increase in attenuation of 0.5dB compared with the uniform lining.

The optimum found for the axially-varying liner illustrates how scattering due to the use of different liners can reduce the noise compared with an uniform liner. The overall increase in the predicted attenuation achieved may appear small (in terms of dB), but it is a 25% increase in ΔPNL over a uniform liner.

VII. Conclusions

In this article the potential benefit of using an axially-varying liner has been demonstrated (at one engine operating condition). The broadband noise attenuation is predicted to be 25% more than for a uniform liner. One aspect of this broadband noise optimization has been the small changes in the objective function with different design configurations. The search was not straightforward, and required more real function evaluations than is usually required. This is mainly due to the nature of the acoustic problem that has been solved. It is likely that a liner optimization based on tonal noise would result in a more well-define set of local optimum points in the design space. Nonetheless the liner optimization process that has been assembled shows the general characteristics that such a procedure should have: versatility; modularity and reliability. The assembled software can be adapted to other types of similar problems. In this case the results suggest that further investigation is required to understand the potential benefit of using an axial liner. The next step in the optimization process will be to include tones, to determine how the optimum liner design is affected by the presence of both tones and broadband noise.

References

[1]J.M. Tyler and T.G. Sofrin. Axial flow compressor noise studies. *Transactions of the Society of AUtomotive Engineers*, 70:309–332, 1962.

[2]W. Eversman G. Zlavog. Source effects on relized attenuation in lined ducts. *9th AIAA/CEAS Aeroacoustics conference and exhibit*, 12-14 May 2003-3247.

[3]J.H. Robinson W.R. Watson. Design and attenuation properties of periodic checkerboard liners. *9th AIAA/CEAS Aeroacoustics conference and exhibit*, 12-14 May 2003-3247.

[4]W. Eversman. Aeroacoustics of flight vehicles: Theory and practice. *NASA RP-1258*, 2(4):681–708, 1991.

[5]D.C. Montgomery R.H. Jones. *Response Surface Methodology: Process and Product Optimization Using Design of Experiments*. Wiley, New York, 1995.

[6]D.R. Jones. A taxonomy of global optimization methods based on response surfaces. *Journal of Global Optimization*, 21:345–383, 2001.

[7]R.E. Kraft R.E. Motsinger. Design performance of duct acoustic treatment. *NASA RP-1258*, 2(4):681–708, 1991.

[8]A. Cumming. High frequency ray acoustics models for duct silencers. *Journal of Sound and Vibration*, 221(4):681–708, 1999.

[9]W.E. Zorumski D.L. Lansing. Effects of wall admittance changes on duct transmission and radiation of sound. *Journal of Sound and Vibration*, 27(1):85–100, 1973.

[10]A.J. Keane. *The Options design exploration system Reference manual and user guide*. 2002.

[11]E.J. Rice. Acoustic liner optimum impedance for spinning modes with mode cutoff ratio as design criterion. *AIAA paper 76-516*, 1979.

[12]C.L. Morfey. Sound transmission and generation in ducts with flow. *Journal of the Acoustic Society of America*, 14(1):37–55, 1971.

[13]W.J. Welch D.R. Jones, M. Schlonlau. Efficient global optimization of expensive black-box function. *Journal of Global Optimization*, 13:445–492, 1998.

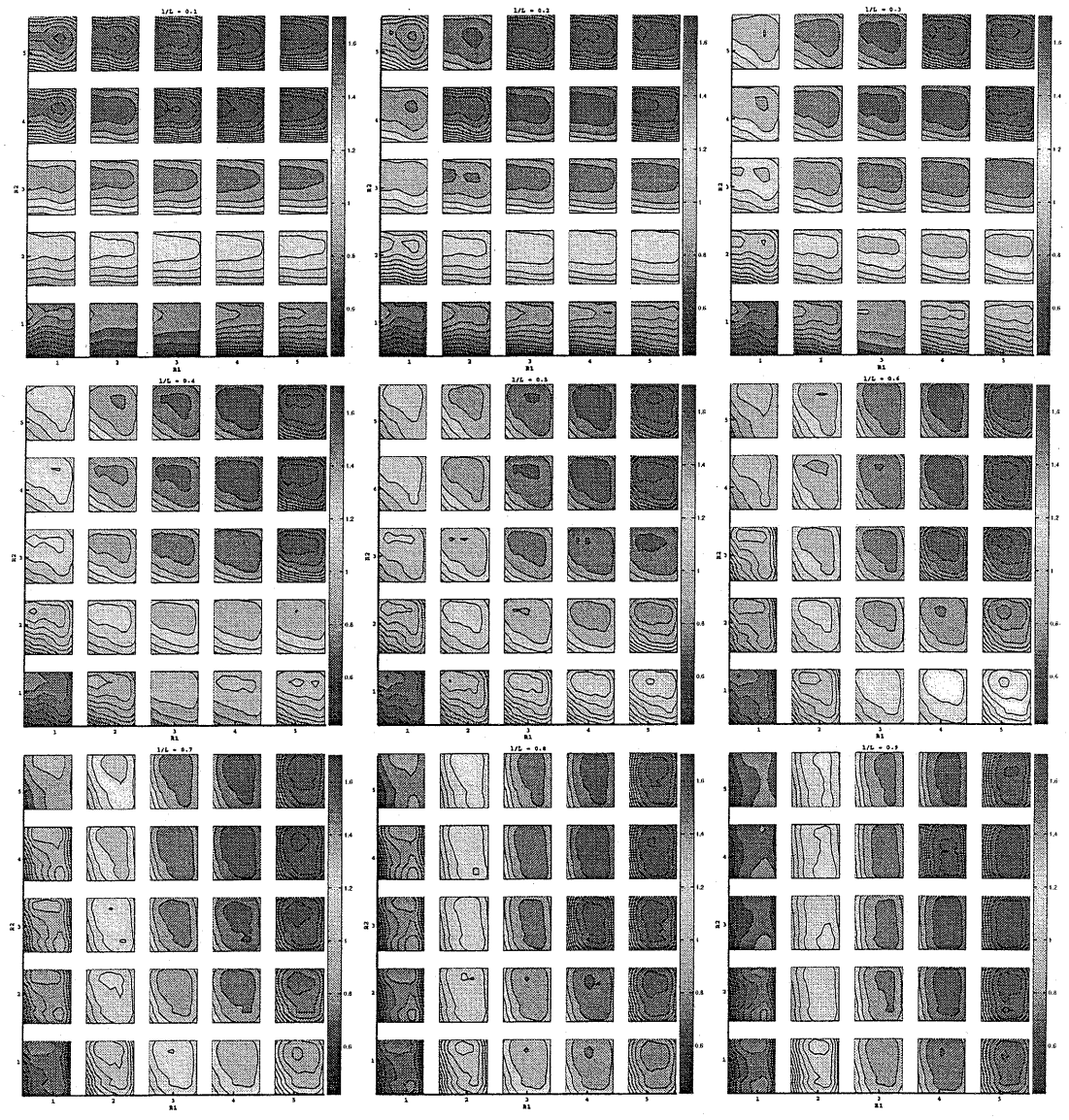

Figure 6. ΔPNL [dB] — axial liner. Different combinations of l_1/L, and R_1, R_2, h_1, h_2.

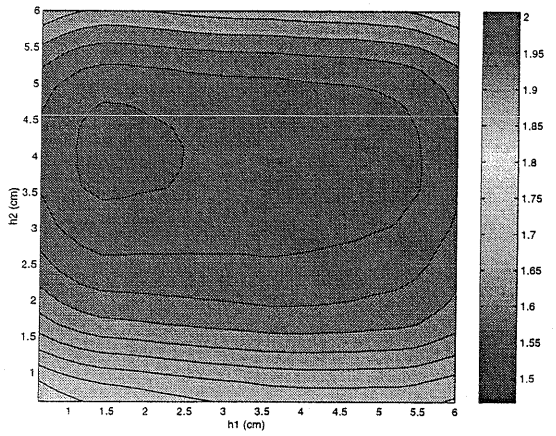

Figure 7. ΔPNL [dB] — axial liner (optimum R_1, R_2 and l_1/L).

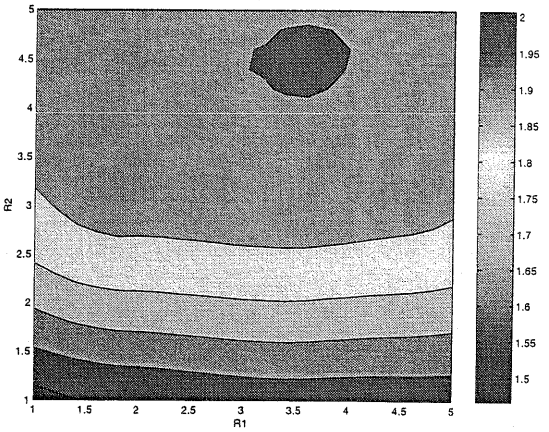

Figure 8. ΔPNL [dB] — axial liner (optimum h_1, h_2 and l_1/L).

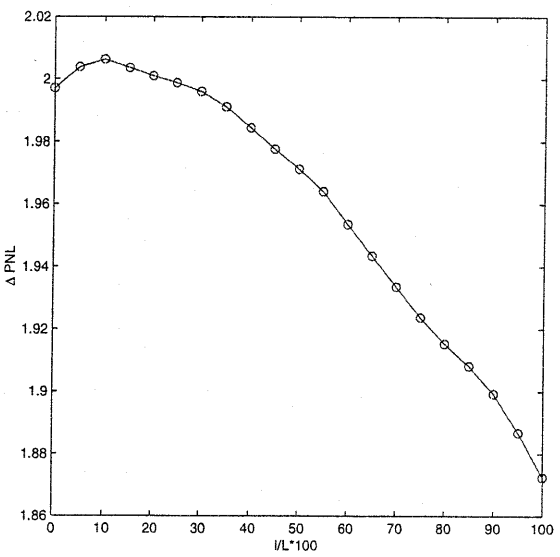

Figure 9. ΔPNL [dB] — axial liner (optimum R_1, R_2, h_1 and h_2).